УДК 519.6:631.4 https://doi.org/10.31713/vt1202514

Shostak L. V., Post-graduate Student (National University of Water and Environmental Engineering, Rivne)

COMPUTER SIMULATION OF TEMPERATURE DISTRIBUTION IN THE FOREST SOIL WITH REGARD TO THE PRESENCE OF A THIN BOUNDARY LAYER OF FALLEN LEAVES

The article addresses the problem of numerical modeling of temperature distribution in the soil of forest ecosystems, taking into account the influence of a thin boundary layer of fallen leaves. This layer significantly alters the thermal conductivity properties of the soil, regulating the heat exchange between the atmosphere and the underlying soil layers. To accurately model the heat exchange processes, the author modified the boundary condition of the heat conduction equation, considering the physical characteristics of the forest litter. The finite difference method was used to solve the corresponding boundary value problem, allowing the variability of heat transfer in the soil to be accounted for. Numerical experiments showed a significant impact of the boundary layer of fallen leaves on the dynamics of temperature changes, which is crucial for assessing ecological processes, improving agricultural technologies, and predicting climate changes. The results obtained can be applied to enhance the understanding of thermal processes in forest ecosystems and develop new approaches to ecological monitoring and climate scenario modeling.

Keywords: **modeling of temperature; soil; forest ecosystem; fallen leaves; thermal insulation; heat transfer; boundary layer; finite difference method; moisture; temperature regime.**

Introduction. The importance of predictive modeling of the state of soil systems in the presence of thin top layers of other materials is dictated by several practically important aspects and the undeniable effects of the influence of such layers on processes in such porous media. In particular, these are: – biofilters for controlling greenhouse gas emissions into the atmosphere from the soil; – the use of mulching in agricultural production; – the use of tillage, in which a layer containing organic residues of the previous crop is formed on top.

Under natural conditions, such layers are present as a product of the ecosystem. In particular, if we take a forest, a layer of fallen leaves and needles creates a thin boundary layer of porous medium with thermal properties that differ from those of the soil and atmosphere. As a result, changes occur in the heat exchange between the soil and the environment, which can affect the soil temperature regime, microbiological processes and hydrological characteristics of the soil profile.

One of the most important areas of use of coatings is their application in landfills to reduce methane emissions. In [1], it was noted that the creation of bio-coating systems is a new methodology for reducing methane (CH_4) emissions from landfills. This study examined the effectiveness of three biosolids systems with different efficiencies in reducing CH_4 emissions from three landfills in Denmark. High CH_4 oxidation efficiencies of more than 95% were found in all systems except one biofilter (55%). Emission measurements over the entire site showed CH_4 emission reduction efficiencies ranging from 29 to 72% after the implementation of biosolids systems at the three landfills, indicating that CH_4 emission reduction is effective.

Paper [2] actually provides an overview of achievements in landfill cover systems. It is noted that municipal solid waste (MSW) landfill cover systems have evolved from simple soil cover to multi-component, nearly impermeable systems that provide better control over infiltration and landfill gas (LFG) emissions. Recently, there has been widespread development of alternative cover systems that address the disadvantages of conventional cover systems, such as high construction and maintenance costs, susceptibility to damage due to cracking from drying and freezing, and ineffective control of LFG emissions. Landfills are considered the third largest source of anthropogenic methane (CH_4) emissions in the United States.

Paper [3] investigated the potential for methane (CH_4) oxidation and sequestration of residual carbon dioxide (CO_2) in a biogeochemical coating system (BGCC) designed to remove CH_4, CO_2, and hydrogen sulfide (H_2S) from LFG emissions.

In agriculture, coatings also have a significant impact on the productivity of agricultural systems. Field experiments [4] have shown that plastic film (PFM) residues can negatively affect soil properties and yields. At the same time, a study [5] demonstrated that mulching with PFM and biodegradable film (BFM) increases yields by 35.4% and 28.3%, respectively, and water use efficiency (WUE) increases by 47.1% and

35.8%. However, such technologies can have an impact on greenhouse gas emissions: according to [6], N_2O emissions from growing potatoes on bare soil were 12.32%–41.03% higher than those of soil with film mulching.

In [7], the results of field experiments on corn fields showed that film mulching increased cumulative CO_2 emissions due to an increase in soil temperature and moisture. Cumulative N_2O emissions were reduced by film mulching. The mulching treatment increased corn yields and improved the net economic budget of the ecosystem, respectively, compared to bare land.

Study [8] shows that plastic mulching increases yields and net economic profit while reducing nitrogen emissions. Study [9] investigated the effects of plastic mulching on the prospects for preserving organic carbon in the soil when nutrient residues from harvesting are returned to the soil. However, the impact of such technologies on greenhouse gas emissions was not studied there. Such studies, based on the analysis of 150 sources, on the impact of mulching on soil organic carbon (SOC) and greenhouse gas emissions are presented in [10]. The authors note that the impact of mulching on SOC and greenhouse gas fluxes differed in different agricultural systems.

In addition to affecting yields and gas emissions, coatings change the temperature regime of the soil. In [11], attention was drawn to differences in air and soil surface temperatures. It is the possibility of such differences that is taken into account in the balance boundary condition [12]. Paper [13] discusses the ROMUL, CENTURY, and ROTHAMSTED models that describe the dynamics of organic residues transformation based on the physicochemical processes of humus formation using differential relations. The results of their practical application are presented, as well as the strengths and weaknesses of each model are highlighted.

An interesting study on the importance of soil surface temperature is presented in [14]. In particular, the authors attempted to trace the relationship between soil surface temperature and groundwater level. This study analyzed the impact of soil surface temperature on changes in groundwater levels in the Bukhara region of Uzbekistan, using data from 1991 to 2020. The results also show that the strength of the relationship between solar radiation and soil surface temperature is very high, with a correlation coefficient of 0.840. The analysis also showed that 53.5% of the changes in groundwater level were observed using the regression model, indicating a moderate correlation between

groundwater level and soil surface temperature. Similarly, work [15] studies the effect of mulching on soil moisture levels.

Paper [16] shows that mulching with black and transparent plastic films significantly increases the yield of spring corn (by 20% on average) compared to bare-soil agricultural technologies. At the same time, [17] noted that mulching with PFM significantly reduced the content of organic matter in the soil and significantly increased the two main greenhouse gas emissions. As a result, film mulching increased the overall global warming potential by 12–82% compared to no mulching, regardless of soil amendments. However, at the same time, yields increased by 8-33%, depending on the conditions. Similarly, [18] showed that CO_2 mulching N_2O with PFM significantly increased the potential CH_4 emissions of CO_2 and N_2O from the soil and contributed to the absorption of CH_4 by the soil.

Modeling soil thermal conductivity with a thin boundary layer of fallen leaves (as an example of a thin layer) is important for a wide range of applications in agronomy and ecology. Accurate representation of the soil temperature regime contributes to more efficient planning of agricultural technologies, such as mulching systems, which help to preserve moisture, optimize heat transfer and improve yields. In the environmental context, taking into account forest litter allows us to assess its role in maintaining microclimate stability, regulating moisture and biogeochemical processes. In addition, the integration of such factors into climate models can improve the accuracy of predicting heat fluxes between the atmosphere and the soil, which is critical for analyzing climate change and developing effective mitigation measures.

Influence of thermophysical properties of soil and boundary layer of fallen leaves on the temperature regime of forest ecosystems. Soil thermal conductivity is a key factor in determining the temperature regime of forest ecosystems. The presence of a thin boundary layer, such as fallen leaves, significantly affects the processes of heat exchange between the atmosphere and the soil.

Various methods and models of soil thermal conductivity [19] take into account its physical properties, such as moisture content, density, and particle size distribution. Studies show that the thermal properties of soils depend on their particle size distribution, moisture [20; 21], density, porosity [22], and organic matter content. In particular, with increasing moisture content, thermal conductivity increases, as water has a higher thermal conductivity compared to the air it displaces from the pores.

The presence of a thin boundary layer, such as fallen leaves, creates additional resistance to heat transfer between the atmosphere and the soil. This layer acts as a thermal insulator, reducing the rate of heat transfer and affecting the temperature regime of the upper soil layers. Studies show that forest plantations reduce the temperature of the soil surface and reduce the amplitude of its fluctuations compared to open areas.

Article [23] presents the results of studies that showed that forest plantations contributed to a decrease in soil temperature. In particular, the surface temperature decreased by 2.7 and 5.3° C, respectively, the temperature at a depth of 50 cm decreased by 1.6 and 2.8° C, and the average temperature of the 0–50 cm layer decreased by 2.5 and 4.5° C, respectively, compared to the southern zonal chernozem. It was also found that the southern zonal chernozem is characterized by sharper temperature fluctuations in the 0–50 cm layer compared to chernozems under forest plantations. In addition, the influence of forest plantations on the southern chernozem led to an increase in the thermophysical characteristics of the upper soil horizons compared to the zonal southern chernozem.

Problem statement in the physical domain. Consider the soil layer Ω (Fig. 1). Above, in contact with the atmosphere, there is a thin boundary layer Ω_δ, the thermophysical characteristics of which differ from those of the soil in the Ω region [12]. It is necessary to build a mathematical model of temperature changes in the soil layer, taking into account the presence of a thin boundary layer, and to study the effect of such a layer on differences in temperature distribution.

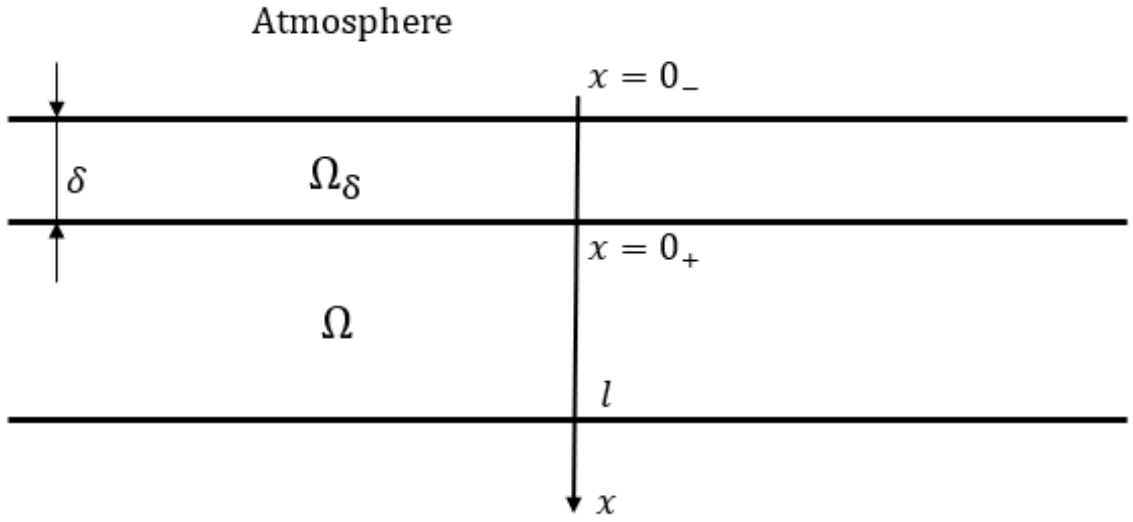

Fig. 1. A soil mass Ω with a thin top layer Ω_δ

Mathematical model of the problem. The mathematical model, when neglecting heat sources, will be described by the following boundary value problem for the heat conduction equation

$$c_v \frac{\partial T(x,t)}{\partial t} = \frac{\partial}{\partial x}\left(\lambda(T)\frac{\partial T(x,t)}{\partial x}\right) - \rho c_\rho u \frac{\partial T(x,t)}{\partial x}, x \in \Omega = (0;l), t > 0, \quad (1)$$

$$T(x,t)|_{t=0} = T_0(x), \qquad x \in \bar{\Omega} = [0;l], \quad (2)$$

$$\lambda(T)\frac{\partial T}{\partial x}\Big|_{x=0} = -\frac{T|_{x=0} - T_a}{\int_0^\delta \frac{dx}{\lambda_\delta(T)}}, \quad (3)$$

Here $c_v = (\rho c_\rho \theta + \rho_a c_a \sigma_a + c_s \rho_s (1 - \theta - \sigma_a))$ is the volumetric heat capacity of the porous medium; c_s is the specific heat capacity of the porous medium skeleton; ρ_s is the density of the porous medium skeleton; θ is the relative humidity; σ_a is the relative air content in the porous medium; ρ_a is the density of air; c_a is the specific heat capacity of air; λ is the thermal conductivity coefficient of the porous medium; ρ is the density of the pore fluid; c_ρ is the specific heat capacity of the pore fluid; T is the temperature; u is the filtration rate of the pore fluid, which in this problem is considered a given function; $\lambda_\delta(T)$ is the thermal conductivity coefficient of the boundary layer material; T_a is the temperature of the atmospheric air above the boundary layer. Condition (3) is a balance boundary condition in the presence of a thin layer and was derived in [12].

Finite difference method. Let us cover the region $\overline{Q}_t = [0;l] \times [0;t]$ with a uniform grid $\overline{Q}_\tau^{(n,m)} = [0;nh] \times [0;m\tau]$ with steps h and τ respectively, in the variable x and time t, where n is the number of steps in the spatial variable, m is the number of steps in time.

To discretize equation (1), we use a monotone difference scheme [24]. As a result, we obtain the following finite difference analog of the differential equation (1)

$$(c_v)_{(i)}^{(j)} \frac{T_i^{(j+1)} - T_i^{(j)}}{\tau} = \frac{\omega_i^{(j)}}{h}\left(\overline{\lambda}_{i+1}^{(j)} \frac{T_{i+1}^{(j+1)} - T_i^{(j+1)}}{h} - \overline{\lambda}_i^{(j)} \frac{T_i^{(j+1)} - T_{i-1}^{(j+1)}}{h}\right) + \rho c_\rho \frac{(u^+)_i^{(j)}}{\lambda_i^{(j)}} \cdot \overline{\lambda}_{i+1}^{(j)} \frac{T_{i+1}^{(j+1)} - T_i^{(j+1)}}{h_2} + \rho c_\rho \frac{(u^-)_i^{(j)}}{\lambda_i^{(j)}} \cdot \overline{\lambda}_i^{(j)} \cdot \frac{T_i^{(j+1)} - T_{i-1}^{(j+1)}}{h_2}, \quad (5)$$

$i = \overline{1, n-1}$, $j = \overline{0, m-1}$.

Here

$$\bar{\lambda}_i^{(j)} = \frac{1}{2} \cdot \left(\lambda_i^{(j)} + \lambda_{i-1}^{(j)}\right), (u^+)_i^{(j)} = \frac{-u_i^{(j)} + \left|u_i^{(j)}\right|}{2} \geq 0,$$

$$(u^-)_i^{(j)} = \frac{-u_i^{(j)} - \left|u_i^{(j)}\right|}{2} \leq 0, \omega_i^{(j)} = \frac{1}{1 + \rho c_\rho \frac{h \cdot \left|u_i^{(j)}\right|}{2 \cdot \lambda_i^{(j)}}} = 1 - \rho c_\rho \frac{h \cdot \left|u_i^{(j)}\right|}{2 \cdot \lambda_i^{(j)}} + O(h^2).$$

Similarly to [24], it can be shown that the differential operators of equation (1) are approximated by the difference operator (5) at any point $(x_i; t_j) \in Q_\tau^{(n;m)}$, $i = \overline{1, n-1}$, $j = \overline{0, m-1}$, with an accuracy of $O(\tau + h^2)$ provided that there exist continuous partial derivatives $\frac{\partial(*)}{\partial \tau}$, $\frac{\partial(*)}{\partial x}$, $\frac{\partial^2(*)}{\partial x^2}$ and piecewise continuous bounded derivatives $\frac{\partial^2(*)}{\partial \tau^2}$, $\frac{\partial^2(*)}{\partial x^2}$ of the function $T(x,t)$, as well as under the condition of the existence of continuous total derivatives $\frac{d(*)}{dx}$ and piecewise continuous bounded derivatives $\frac{d^2(*)}{dx^2}$ of the function λ and derivatives $\frac{d(*)}{d\tau}$ of the functions λ, $\frac{d\lambda}{dx}$.

The system of linear algebraic equations (5) is linear with respect to the desired values of the function $T(x,t)$.

To find the temperature $T(x,t)$ from the system of linear algebraic equations (5), we use the method of running [23]. To do this, we write this equation in the running form

$$a_i \cdot T_{i-1}^{(j+1)} - c_i \cdot T_i^{(j+1)} + b_i \cdot T_{i+1}^{(j+1)} = -T_i^{(j)},$$

where

$$a_i = \frac{\tau}{c_v} \cdot \frac{\bar{\lambda}_i^{(j)}}{h} \cdot \left(\frac{\omega_i^{(j)}}{h} - \frac{\rho c_\rho (u^-)_i^{(j)}}{\lambda_i^{(j)}}\right), b_i = \frac{\tau}{c_v} \cdot \frac{\bar{\lambda}_{i+1}^{(j)}}{h} \cdot \left(\frac{\omega_i^{(j)}}{h} + \frac{\rho c_\rho (u^+)_i^{(j)}}{\lambda_i^{(j)}}\right),$$

$$c_i = 1 + \frac{\tau}{c_v}\left(\frac{\omega_i^{(j)} \cdot (\bar{\lambda}_{i+1}^{(j)} + \bar{\lambda}_i^{(j)})}{h^2} + \frac{\rho c_\rho}{h \lambda_i^{(j)}} \cdot \left((u^+)_i^{(j)} \cdot \bar{\lambda}_{i+1}^{(j)} - (u^-)_i^{(j)} \cdot \bar{\lambda}_i^{(j)}\right)\right).$$

The conditions $|c_i| \geq |a_i| + |b_i|$ of run stability are met.

The temperature value at the time layer $(j+1)$ is consistently found

using the following relation

$$T_i^{(j+1)} = \alpha_{i+1} \cdot T_{i+1}^{(j+1)} + \beta_{i+1}, \quad (6)$$

where

$$\alpha_{i+1} = \frac{b_i}{c_i - a_i\alpha_i}, \qquad \beta_{i+1} = \frac{a_i\beta_i + c_i^{(j)} + s_i^{(j+1)}}{c_i - a_i\alpha_i}.$$

For the initial conditions (2), we obtain the following finite difference analogs

$$T_i^{(0)} = T_0(ih), \quad i = \overline{0,n}. \tag{7}$$

Let us approximate the boundary condition (3). Consider the expression

$$\frac{1}{2}\left(\lambda_1^{(j)} + \lambda_0^{(j)}\right)\frac{T_1^{(j+1)} - T_0^{(j+1)}}{h} = \frac{1}{2}\left(2\lambda_0^{(j)} + h\frac{\partial\lambda}{\partial x}\Big|_{x_0}^{t_{j+1}} + O(h^2)\right)\times$$

$$\times\frac{T_0^{(j+1)} + h\frac{\partial T}{\partial x}\Big|_{x_0}^{t_{j+1}} + \frac{1}{2}h^2\frac{\partial^2 T}{\partial x^2}\Big|_{x_0}^{t_{j+1}} + O(h^3) - T_0^{(j+1)}}{h} =$$

$$= \frac{1}{2}\left(2\lambda_0^{(j)} + h\frac{\partial\lambda}{\partial x}\Big|_{x_0}^{t_{j+1}} + O(h^2)\right)\left(\frac{\partial T}{\partial x}\Big|_{x_0}^{t_{j+1}} + \frac{1}{2}h\frac{\partial^2 T}{\partial x^2}\Big|_{x_0}^{t_{j+1}} + O(h^2)\right) =$$

$$= \lambda_0^{(j)}\frac{\partial T}{\partial x}\Big|_{x_0}^{t_{j+1}} + 0.5h\frac{\partial}{\partial x}\left(\lambda\frac{\partial T}{\partial x}\right)\Big|_{x_0}^{t_{j+1}} + O(h^2).$$

From the above expression we get

$$\lambda_0^{(j)}\frac{\partial T}{\partial x}\Big|_{x_0}^{t_{j+1}} = \overline{\lambda}_1^{(j)}\frac{T_1^{(j+1)} - T_0^{(j+1)}}{h} - 0.5h\frac{\partial}{\partial x}\left(\lambda\frac{\partial T}{\partial x}\right)\Big|_{x_0}^{t_{j+1}} + O(h^2). \tag{8}$$

Then from equation (1) we have

$$\frac{\partial}{\partial x}\left(\lambda\frac{\partial T(x,t)}{\partial x}\right) = c_v\frac{\partial T(x,t)}{\partial t} + \rho c_p u\frac{\partial T(x,t)}{\partial x}.$$

Substituting this expression into (8), we obtain

$$\lambda_0^{(j)}\frac{\partial T}{\partial x}\Big|_{x_0}^{t_{j+1}} = \overline{\lambda}_1^{(j)}\frac{T_1^{(j+1)} - T_0^{(j+1)}}{h} - 0.5h\left(c_v\frac{\partial T}{\partial t} + \rho c_p u\frac{\partial T}{\partial x}\right)\Big|_{x_0}^{t_{j+1}} + O(h^2). \tag{9}$$

Next, using the approximation

$$\left(-u\frac{\partial T}{\partial x}\right)\Big|_{x_0}^{t_{j+1}} = (u^+)_0^{(j)}T_{\overline{x},0}^{(j+1)} + (u^-)_0^{(j)}T_{x,0}^{(j+1)} + O(\tau + h)$$

from (9) we obtain

$$\left(\lambda_0^{(j)} - 0.5h\rho c_p(u^-)_0^{(j)}\right)\frac{\partial T}{\partial x}\Big|_{x_0}^{t_{j+1}} = \overline{\lambda}_1^{(j)}\frac{T_1^{(j+1)} - T_0^{(j+1)}}{h} -$$

$$-0.5hc_v\frac{T_0^{(j+1)}-T_0^{(j)}}{\tau}+0.5h(u^+)_0^{(j)}\frac{T_1^{(j+1)}-T_0^{(j+1)}}{h}+O(h^2). \qquad (10)$$

Thus, from the boundary condition (3), we obtain its approximation with an accuracy of $O(\tau+h^2)$

$$-\left(\lambda_0^{(j)}-0.5h\rho c_p(u^-)_0^{(j)}\right)\frac{T_0^{(j+1)}-T_a}{\lambda_0^{(j)}\int_0^{\delta}\frac{dx}{\lambda_\delta(T^{(j)})}}=\bar{\lambda}_1^{(j)}\frac{T_1^{(j+1)}-T_0^{(j+1)}}{h}-$$

$$-0.5hc_v\frac{T_0^{(j+1)}-T_0^{(j)}}{\tau}+0.5h(u^+)_0^{(j)}\frac{T_1^{(j+1)}-T_0^{(j+1)}}{h}+O(\tau+h^2). \qquad (11)$$

From (11) we obtain

$$\frac{\left(\lambda_0^{(j)}-0.5h\rho c_p(u^-)_0^{(j)}\right)T_a}{\lambda_0^{(j)}\int_0^{\delta}\frac{dx}{\lambda_\delta(T^{(j)})}}-0.5hc_v\frac{T_0^{(j)}}{\tau}=$$

$$=\left(\frac{\lambda_0^{(j)}-0.5h\rho c_p(u^-)_0^{(j)}}{\lambda_0^{(j)}\int_0^{\delta}\frac{dx}{\lambda_\delta(T^{(j)})}}-\frac{\bar{\lambda}_1^{(j)}}{h}-\frac{0.5hc_v}{\tau}-0.5(u^+)_0^{(j)}\right)T_0^{(j+1)}+$$

$$+\left(\bar{\lambda}_1^{(j)}\frac{T_1^{(j+1)}}{h}+0.5h(u^+)_0^{(j)}\frac{T_1^{(j+1)}}{h}\right)T_1^{(j+1)}$$

or

$$T_0^{(j+1)}=\alpha_1\cdot T_1^{(j+1)}+\beta_1,$$

where

$$\alpha_1=\frac{\alpha_{up}}{\alpha},\beta_1=\frac{\beta_{up}}{\alpha},\alpha_{up}=\bar{\lambda}_1^{(j)}\frac{T_1^{(j+1)}}{h}+0.5h(u^+)_0^{(j)}\frac{T_1^{(j+1)}}{h},$$

$$\beta_{up}=-\frac{\left(\lambda_0^{(j)}-0.5h\rho c_p(u^-)_0^{(j)}\right)T_a}{\lambda_0^{(j)}\int_0^{\delta}\frac{dx}{\lambda_\delta(T^{(j)})}}+0.5hc_v\frac{T_0^{(j)}}{\tau},$$

$$\alpha=-\frac{\lambda_0^{(j)}-0.5h\rho c_p(u^-)_0^{(j)}}{\lambda_0^{(j)}\int_0^{\delta}\frac{dx}{\lambda_\delta(T^{(j)})}}+\frac{\bar{\lambda}_1^{(j)}}{h}+\frac{0.5hc_v}{\tau}+0.5(u^+)_0^{(j)}.$$

So, using the run method, we obtained the expressions for α_1,β_1.

Results of numerical experiments. To evaluate the effect of a thin boundary layer of fallen leaves on the temperature distribution in the forest soil, numerical experiments were conducted using a thermal conductivity model that takes into account the thermal properties of the

soil and the presence of organic cover [25; 26].

The calculations were performed for different seasonal conditions and soil moisture, taking into account changes in atmospheric temperature. The initial atmospheric temperature used in the experiments was 20° C.

For numerical experiments, the following parameter values were set $\lambda = 0{,}47\frac{W}{mK}$ and $\lambda_\delta = 0{,}2\frac{W}{mK}$ (Fig. 2, Fig. 3). For Figure 4, the following thermal conductivity values were used: $\lambda_\delta = 0{,}2\frac{W}{mK}$, clay $\lambda = 0{,}25\frac{W}{mK}$, peat $\lambda = 0{,}15\frac{W}{mK}$, sand $\lambda = 0{,}47\frac{W}{mK}$. Based on the numerical experiments (Fig. 2, Fig. 3, Fig. 4), it was found that the presence of a thin boundary layer of fallen leaves significantly affects the soil temperature regime. For all depths, temperature curves with the presence of leaves show a lower rate of soil heating compared to areas without leaves. The most significant difference is observed in the upper layers (0.2-0.6 m), where fallen leaves act as a heat-insulating layer, reducing the rate of heat transfer from the atmosphere to the soil. In the deeper layers (0.8-1.0 m), the insulation effect gradually decreases, but the temperature in these horizons is still slightly lower in cases with leaves. This confirms the hypothesis that fallen leaves play a key role in regulating soil temperature in forest ecosystems.

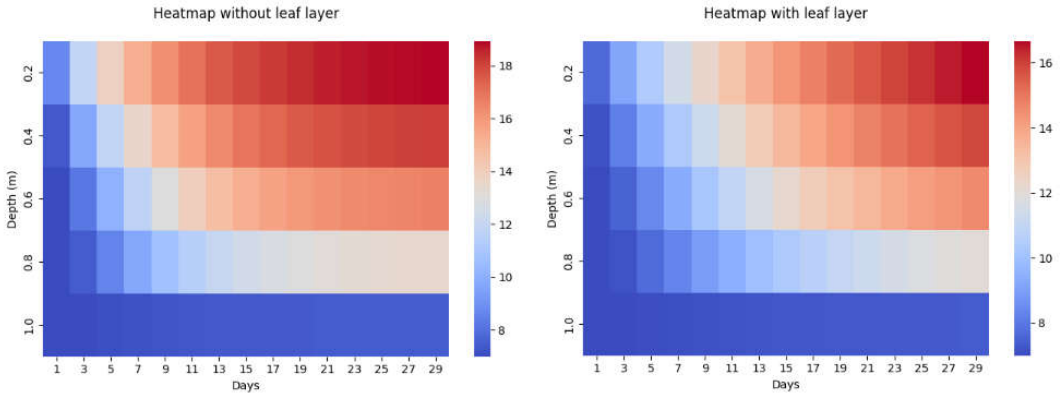

Fig. 2. Heat maps of temperature distribution in sand soil with and without fallen leaves

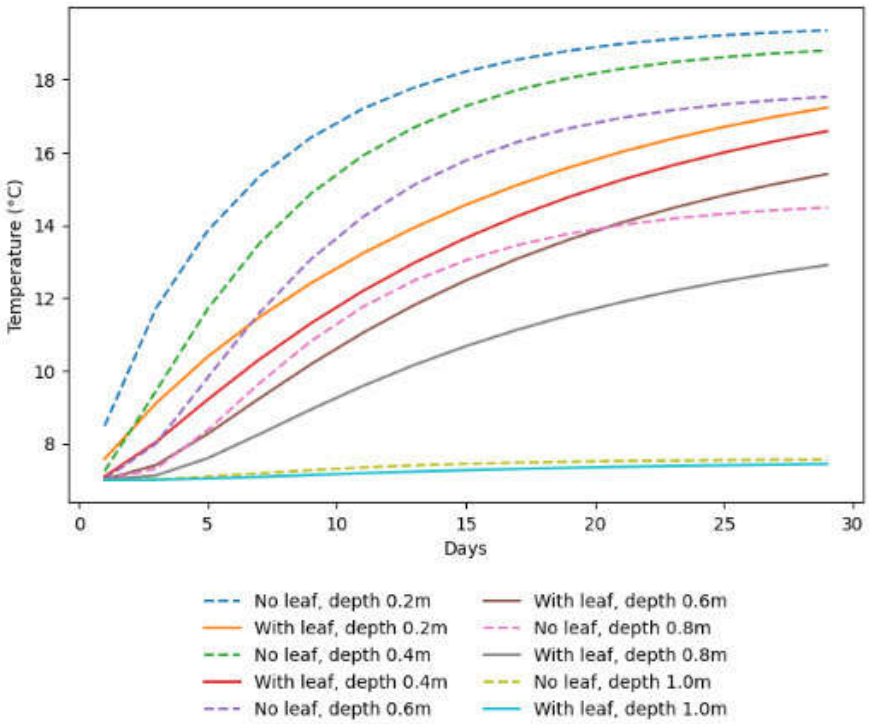

Fig. 3. Influence of the boundary layer of fallen leaves in loamy sand soil on soil temperature changes

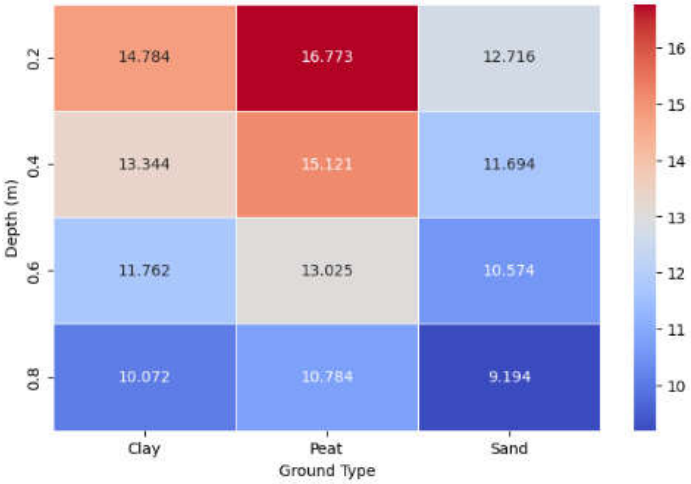

Fig. 4. Temperature distribution in different soil types on the 10th day of modeling in the presence of a thin layer

The following parameters were used for Figure 5: $\lambda = 0{,}44\frac{W}{mK}$, dry oak leaves $\lambda_\delta = 0{,}08\frac{W}{mK}$, wet oak leaves $\lambda_\delta = 0{,}12\frac{W}{mK}$, pine needles $\lambda_\delta = 0{,}05\frac{W}{mK}$, birch leaves $\lambda_\delta = 0{,}1\frac{W}{mK}$. For Figure 6 oak leaves $\lambda_\delta = 0{,}08\frac{W}{mK}$. Figures (Fig. 5, Fig. 6) show the results of modeling the temperature change along the depth of the sandy loam soil depending on the type and thickness of the boundary layer of fallen leaves. As can

be seen, different types of leaves demonstrate variations in the thermal insulation effect, which affects the temperature of the upper soil layers. Increasing the thickness of the leaf layer also helps to reduce heat loss, which is consistent with the established relationship between the parameters of the boundary layer and its insulating effect.

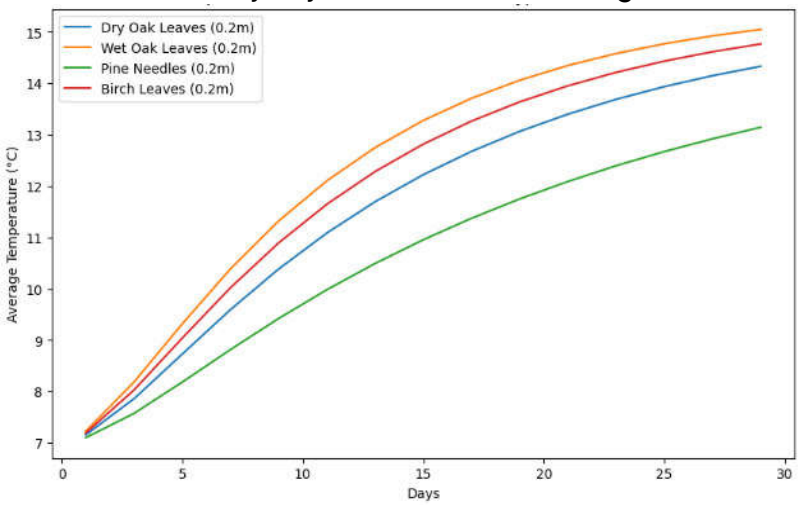

Fig. 5. Changes in loamy sand soil temperature under different types of fallen leaves

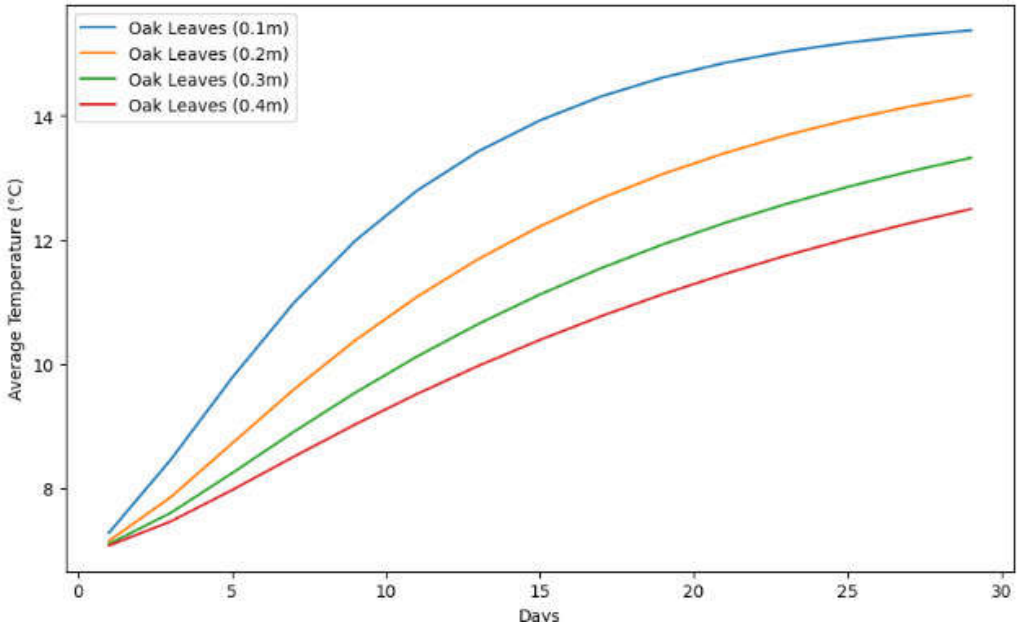

Fig. 6. Changes in soil temperature in loamy sand with different thicknesses of fallen oak leaves

Figure 7 illustrates the average soil temperature in the presence of oak leaves with different moisture levels. Numerical experiments revealed that the thermal conductivity of the organic layer significantly influences the soil temperature dynamics.

To model this dependency, the thermal conductivity (λ) was assumed to be a function of soil volumetric water content (θ), using an interpolation between the dry and saturated thermal conductivities [27]:

$$\lambda(\theta) = \lambda_{dry} + (\lambda_{sat} - \lambda_{dry})(\theta/\theta_s)^{0.5},$$

where λ_{dry} represents the thermal conductivity of dry oak leaves and λ_{sat} corresponds to that of fully saturated leaves and θ_s is saturated water content. This approach accounts for the gradual increase in thermal conductivity with moisture content, reflecting the reduced insulating properties of wet leaves.

The results indicate that wetter oak leaves lead to higher soil temperatures, as their increased thermal conductivity allows more efficient heat transfer from the atmosphere to the soil. In contrast, dry oak leaves act as a stronger insulator, reducing heat penetration and leading to lower soil temperatures. Under the wettest conditions, the soil temperature closely follows atmospheric temperature variations, whereas the dry leaf layer maintains a cooler soil environment.

These findings highlight the importance of considering the moisture content of the organic layer when predicting the thermal regime of forest soils. Neglecting this factor could lead to significant inaccuracies in modeling soil temperature dynamics, particularly in ecosystems with substantial organic cover.

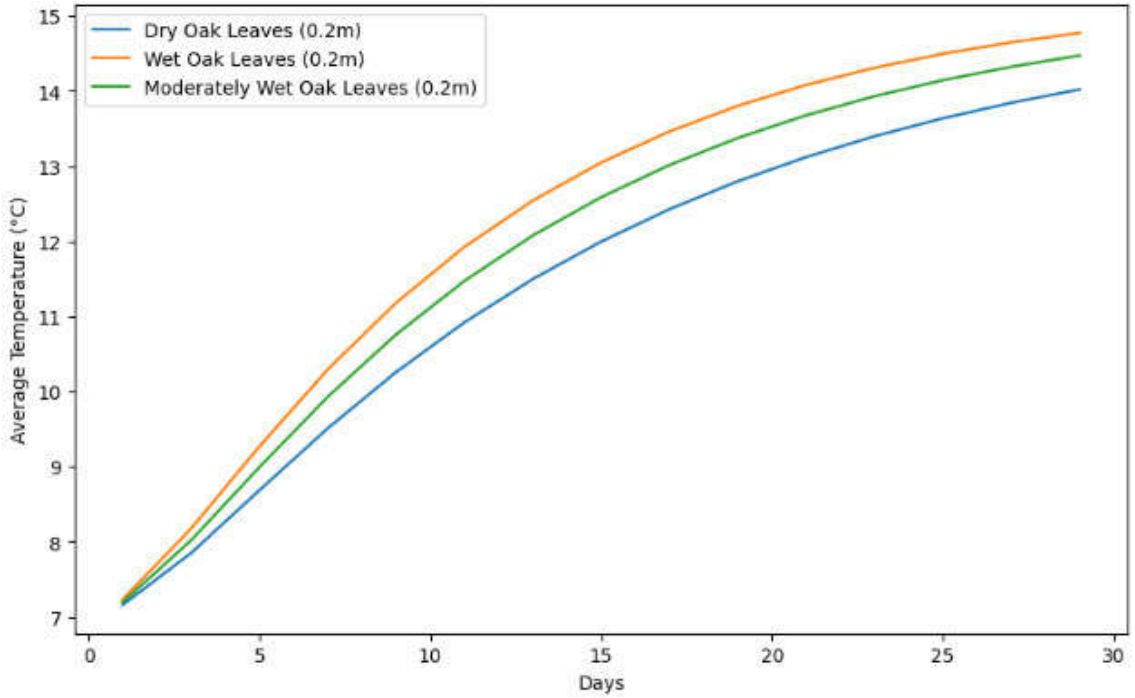

Fig. 7. Temperature variation with different moisture levels of oak leaves

The results obtained can be used to improve models for predicting the temperature regime of forest ecosystems, as well as for environmental planning and management of forest resources.

Conclusion. The article deals with the problem of modeling the temperature distribution in the soil of a forest ecosystem, taking into account the influence of a thin boundary layer of fallen leaves. To build a mathematical model of heat transfer, the boundary conditions of the heat conduction equation were modified, which allowed us to take into account the physical characteristics of the forest floor and its thermal insulation properties.

Numerical solutions obtained using the finite difference method showed a significant influence of the layer of fallen leaves on the soil temperature regime. It was found that the presence of leaves reduces the rate of soil heating, especially in the upper layers, where fallen leaves act as a thermal insulation layer. This reduces the rate of heat transfer from the atmosphere to the soil and ensures a more stable temperature in these layers.

The analysis of the results of numerical experiments also showed that the thickness and moisture content of the boundary layer have a significant impact on soil temperature. Increasing the thickness of the leaf layer reduces heat loss, which confirms the relationship between the layer parameters and its insulating effect. Wet leaves reduce thermal insulation properties, which causes an increase in soil temperature compared to dry leaves.

The results emphasize the importance of taking into account heat and moisture exchange in modeling the temperature regime of forest soil. This allows for more accurate predictions of temperature dynamics, which is important for ecological research, agricultural technology, and climate change forecasting in forest ecosystems.

1. Duan Z., Scheutz C., Kjeldsen P. Mitigation of methane emissions from three Danish landfills using different biocover systems. *Waste Management*. 2022. Vol. 149. Pp. 156–167. https://doi.org/10.1016/j.wasman.2022.05.022. **2.** Chetri J. K., Reddy K. R. Advancements in municipal solid waste landfill cover system: a review. *J Indian Inst Sci*. 2021. Vol. 101. Pp. 557–588. URL: https://doi.org/10.1007/s41745-021-00229-1. **3.** Verma G., Chetri J. K., Reddy K. R. Spatial variation of methane oxidation and carbon dioxide sequestration in landfill biogeochemical cover. *Environmental Technology*. 2024. URL: https://doi.org/10.1080/09593330.2024.2372052. **4.** Uzamurera A. G., Zhao Z.-Y., Wang P.-Y., Wei Y.-X., Mo F., Zhou R., Wang W.-L., Ullah F., Khan A., Xiong X.-B., Li M.-Y., Wesly K., Wang W.-Y., Tao H.-Y., Xiong Y.-C. Thickness effects of

polyethylene and biodegradable film residuals on soil properties and dryland maize productivity. *Chemosphere*. 2023. Vol. 329. P. 138602. URL: https://doi.org/10.1016/j.chemosphere.2023.138602. **5.** Chen N., Li X., Shi H., Yan J., Hu Q., Zhang Y. Assessment and modeling of maize evapotranspiration and yield with plastic and biodegradable film mulch. *Agricultural and Forest Meteorology*. 2021. Vol. 307. P. 108474. URL: https://doi.org/10.1016/j.agrformet.2021.108474. **6.** Wang W., Han L., Zhang X., Wei K. Plastic film mulching affects N2O emission and ammonia oxidizers in drip-irrigated potato soil in northwest China. *Science of The Total Environment*. 2021. Vol. 754. P. 142113. URL: https://doi.org/10.1016/j.scitotenv.2020.142113. **7.** Zhang W., Gu J., Zhang Y., Chen Z., Zhu Z., Liu Y., Sun S. Effects of PBAT/PLA biodegradable film mulching on greenhouse gas emissions in rain-fed maize farmland of Northeast China. Science of The Total Environment. 2024. Vol. 957. P. 177725. https://doi.org/10.1016/j.scitotenv.2024.177725. **8.** Wang L., Coulter J.A., Li L., Luo Z., Chen Y., Deng X., Xie J. Plastic mulching reduces nitrogen footprint of food crops in China: a meta-analysis. *Science of The Total Environment*. 2020. Vol. 748. P. 141479. URL: https://doi.org/10.1016/j.scitotenv.2020.141479. **9.** Quan H., Wang B., Wu L., Feng H., Wu L., Wu L., Liu D. L., Siddique K. H. M. Impact of plastic mulching and residue return on maize yield and soil organic carbon storage in irrigated dryland areas under climate change. *Agriculture, Ecosystems & Environment*. 2024. Vol. 362. P. 108838. URL: https://doi.org/10.1016/j.agee.2023.108838. **10.** Yu Y., Zhang Y., Xiao M., Zhao C., Yao H. A meta-analysis of film mulching cultivation effects on soil organic carbon and soil greenhouse gas fluxes. *CATENA*. 2021. Vol. 206. P. 105483. URL: https://doi.org/10.1016/j.catena.2021.105483. **11.** Molnar P. Differences between soil and air temperatures: Implications for geological reconstructions of past climate. *Geosphere*. 2022. Vol. 18. Issue 2. Pp. 800–824. URL: https://doi.org/10.1130/GES02448.1. **12.** Stepanchenko O., Martyniuk P., Belozerova O., Shostak L. Balance boundary conditions for thin boundary layers: derivation from the integral conjugation conditions. *International Journal of Applied Mathematics*. 2023. Vol. 36. Issue 1. Pp. 107–116. URL: https://doi.org/10.12732/ijam.v36i1.9. **13.** Shostak L., Boiko M., Stepanchenko O., Kozhushko O. Analysis of soil organic matter transformation dynamics models. *Informatyka, Automatyka, Pomiary w Gospodarce i Ochronie Środowiska*. 2019. Vol. 9. Pp. 40–45. **14.** Khamidov M., Ishchanov J., Hamidov A., Shermatov E., Gafurov Z. Impact of soil surface temperature on changes in the groundwater level. *Water*. 2023. Vol. 15. Issue 21. Pp. 3865. URL: https://doi.org/10.3390/w15213865. **15.** Jia Q., Shi H., Li R., Miao Q., Feng Y., Wang N., Li J. Evaporation of maize crop under mulch film and soil covered drip irrigation: field assessment and modelling on West Liaohe Plain, China. *Agricultural Water Management*. 2021. Vol. 253. P. 106894. URL: https://doi.org/10.1016/j.agwat.2021.106894. **16.** Li C., Wang Q., Wang N., Luo X., Li Y., Zhang T., Feng H., Dong Q. Effects of different plastic film mulching on soil

hydrothermal conditions and grain-filling process in an arid irrigation district. *Science of The Total Environment*. 2021. Vol. 795. P. 148886. https://doi.org/10.1016/j.scitotenv.2021.148886. **17.** Cuello J. P., Hwang H. Y., Gutierrez J., Kim S. Y., Kim P. J. Impact of plastic film mulching on increasing greenhouse gas emissions in temperate upland soil during maize cultivation. *Applied Soil Ecology*. 2015. Vol. 91. Pp. 48–57. URL: https://doi.org/10.1016/j.apsoil.2015.02.007. **18.** Nan W., Yue S., Huang H., Li S., Shen Y. Effects of plastic film mulching on soil greenhouse gases (CO2, CH4 and N2O) concentration within soil profiles in maize fields on the Loess Plateau, China. *Journal of Integrative Agriculture*. 2016. Vol. 15. Issue 2. Pp. 451–464. URL: https://doi.org/10.1016/S2095-3119(15)61106-6. **19.** Dai Y., Wei N., Yuan H., Zhang S., Shangguan W., Liu S., Lu X., Xin Y. Evaluation of soil thermal conductivity schemes for use in land surface modeling. *Journal of Advances in Modeling Earth Systems*. 2019. https://doi.org/10.1029/2019MS001723. **20.** Lunt P. H., Fuller K., Fox M., Goodhew S., Murphy T. R. Comparing the thermal conductivity of three artificial soils under differing moisture and density conditions for use in green infrastructure. *Soil Use and Management*. 2022. Vol. 39. Issue 1. Pp. 260–269. URL: https://doi.org/10.1111/sum.128415. **21.** Zhu X., Gao Z., Chen T., Wang W., Lu C., Zhang Q. Study on the thermophysical properties and influencing factors of regional surface shallow rock and soil in China. *Frontiers in Earth Science*. 2022. Vol. 10. P. 864548. URL: https://doi.org/10.3389/feart.2022.864548. **22.** Petcu C., Dobrescu C. F., Dragomir C. S., Ciobanu A. A., Lăzărescu A. V., Hegyi A. Thermophysical Characteristics of Clay for Efficient Rammed Earth Wall Construction. *Materials*. 2023. Vol. 16. Issue 17. P. 6015. URL: https://doi.org/10.3390/ma16176015. **23.** Gorban V. A., Bilova N. A. Forest plantations influence on the thermophysical properties of southern chernozems. *Visnyk of V. N. Karazin Kharkiv National University. Series Ecology*. 2024. Issue 30. URL: https://doi.org/10.26565/1992-4259-2024-30-02. **24.** Vlasyuk A., Zhukovskyy V., Zhukovska N., Pinchuk O., Rajab H. Mathematical modeling of heat, mass, and moisture transfer in catalytic porous media. *WSEAS Transactions on Applied and Theoretical Mechanics*. 2020. May. URL: https://doi.org/10.37394/232011.2020.15.8. **25.** Nikiforova T., Savytskyi M., Limam K., Bosschaerts W., Belarbi R. Methods and results of experimental researches of thermal conductivity of soils. *Energy Procedia*. 2013. Vol. 42. Pp. 775–783. URL: https://doi.org/10.1016/j.egypro.2013.12.034. **26.** Sadeghi M., Ghanbarian B., Horton R. Derivation of an explicit form of the percolation-based effective-medium approximation for thermal conductivity of partially saturated soils. *Water Resources Research*. 2018. Vol. 54. Pp. 1389–1399. URL: https://doi.org/10.1002/2017WR021714. **27.** Somerton W. H., El-Shaarani A. H., Mobarak S. M. High temperature behavior of rocks associated with geothermal type reservoirs. *Paper SPE-4897 presented at 44th Annual California Regional Meeting of the Society of Petroleum Engineers*. San Francisco, CA, 1974. URL: https://doi.org/10.2118/4897-MS

REFERENCES:

1. Duan Z., Scheutz C., Kjeldsen P. Mitigation of methane emissions from three Danish landfills using different biocover systems. *Waste Management*. 2022. Vol. 149. Pp. 156–167. https://doi.org/10.1016/j.wasman.2022.05.022. **2.** Chetri J. K., Reddy K. R. Advancements in municipal solid waste landfill cover system: a review. *J Indian Inst Sci*. 2021. Vol. 101. Pp. 557–588. URL: https://doi.org/10.1007/s41745-021-00229-1. **3.** Verma G., Chetri J. K., Reddy K. R. Spatial variation of methane oxidation and carbon dioxide sequestration in landfill biogeochemical cover. *Environmental Technology*. 2024. URL: https://doi.org/10.1080/09593330.2024.2372052. **4.** Uzamurera A. G., Zhao Z.-Y., Wang P.-Y., Wei Y.-X., Mo F., Zhou R., Wang W.-L., Ullah F., Khan A., Xiong X.-B., Li M.-Y., Wesly K., Wang W.-Y., Tao H.-Y., Xiong Y.-C. Thickness effects of polyethylene and biodegradable film residuals on soil properties and dryland maize productivity. *Chemosphere*. 2023. Vol. 329. P. 138602. URL: https://doi.org/10.1016/j.chemosphere.2023.138602. **5.** Chen N., Li X., Shi H., Yan J., Hu Q., Zhang Y. Assessment and modeling of maize evapotranspiration and yield with plastic and biodegradable film mulch. *Agricultural and Forest Meteorology*. 2021. Vol. 307. P. 108474. URL: https://doi.org/10.1016/j.agrformet.2021.108474. **6.** Wang W., Han L., Zhang X., Wei K. Plastic film mulching affects N2O emission and ammonia oxidizers in drip-irrigated potato soil in northwest China. *Science of The Total Environment*. 2021. Vol. 754. P. 142113. URL: https://doi.org/10.1016/j.scitotenv.2020.142113. **7.** Zhang W., Gu J., Zhang Y., Chen Z., Zhu Z., Liu Y., Sun S. Effects of PBAT/PLA biodegradable film mulching on greenhouse gas emissions in rain-fed maize farmland of Northeast China. Science of The Total Environment. 2024. Vol. 957. P. 177725. https://doi.org/10.1016/j.scitotenv.2024.177725. **8.** Wang L., Coulter J.A., Li L., Luo Z., Chen Y., Deng X., Xie J. Plastic mulching reduces nitrogen footprint of food crops in China: a meta-analysis. *Science of The Total Environment*. 2020. Vol. 748. P. 141479. URL: https://doi.org/10.1016/j.scitotenv.2020.141479. **9.** Quan H., Wang B., Wu L., Feng H., Wu L., Wu L., Liu D. L., Siddique K. H. M. Impact of plastic mulching and residue return on maize yield and soil organic carbon storage in irrigated dryland areas under climate change. *Agriculture, Ecosystems & Environment*. 2024. Vol. 362. P. 108838. URL: https://doi.org/10.1016/j.agee.2023.108838. **10.** Yu Y., Zhang Y., Xiao M., Zhao C., Yao H. A meta-analysis of film mulching cultivation effects on soil organic carbon and soil greenhouse gas fluxes. *CATENA*. 2021. Vol. 206. P. 105483. URL: https://doi.org/10.1016/j.catena.2021.105483. **11.** Molnar P. Differences between soil and air temperatures: Implications for geological reconstructions of past climate. *Geosphere*. 2022. Vol. 18. Issue 2. Pp. 800–824. URL: https://doi.org/10.1130/GES02448.1. **12.** Stepanchenko O., Martyniuk P., Belozerova O., Shostak L. Balance boundary conditions for thin boundary layers: derivation from the integral conjugation conditions. *International Journal of Applied Mathematics*. 2023. Vol. 36. Issue 1. Pp. 107–116. URL: https://doi.org/10.12732/ijam.v36i1.9. **13.** Shostak L., Boiko M., Stepanchenko

O., Kozhushko O. Analysis of soil organic matter transformation dynamics models. *Informatyka, Automatyka, Pomiary w Gospodarce i Ochronie Środowiska*. 2019. Vol. 9. Pp. 40–45. **14.** Khamidov M., Ishchanov J., Hamidov A., Shermatov E., Gafurov Z. Impact of soil surface temperature on changes in the groundwater level. *Water*. 2023. Vol. 15. Issue 21. Pp. 3865. URL: https://doi.org/10.3390/w15213865. **15.** Jia Q., Shi H., Li R., Miao Q., Feng Y., Wang N., Li J. Evaporation of maize crop under mulch film and soil covered drip irrigation: field assessment and modelling on West Liaohe Plain, China. *Agricultural Water Management*. 2021. Vol. 253. P. 106894. URL: https://doi.org/10.1016/j.agwat.2021.106894. **16.** Li C., Wang Q., Wang N., Luo X., Li Y., Zhang T., Feng H., Dong Q. Effects of different plastic film mulching on soil hydrothermal conditions and grain-filling process in an arid irrigation district. *Science of The Total Environment*. 2021. Vol. 795. P. 148886. https://doi.org/10.1016/j.scitotenv.2021.148886. **17.** Cuello J. P., Hwang H. Y., Gutierrez J., Kim S. Y., Kim P. J. Impact of plastic film mulching on increasing greenhouse gas emissions in temperate upland soil during maize cultivation. *Applied Soil Ecology*. 2015. Vol. 91. Pp. 48–57. URL: https://doi.org/10.1016/j.apsoil.2015.02.007. **18.** Nan W., Yue S., Huang H., Li S., Shen Y. Effects of plastic film mulching on soil greenhouse gases (CO2, CH4 and N2O) concentration within soil profiles in maize fields on the Loess Plateau, China. *Journal of Integrative Agriculture*. 2016. Vol. 15. Issue 2. Pp. 451–464. URL: https://doi.org/10.1016/S2095-3119(15)61106-6. **19.** Dai Y., Wei N., Yuan H., Zhang S., Shangguan W., Liu S., Lu X., Xin Y. Evaluation of soil thermal conductivity schemes for use in land surface modeling. *Journal of Advances in Modeling Earth Systems*. 2019. https://doi.org/10.1029/2019MS001723. **20.** Lunt P. H., Fuller K., Fox M., Goodhew S., Murphy T. R. Comparing the thermal conductivity of three artificial soils under differing moisture and density conditions for use in green infrastructure. *Soil Use and Management*. 2022. Vol. 39. Issue 1. Pp. 260–269. URL: https://doi.org/10.1111/sum.128415. **21.** Zhu X., Gao Z., Chen T., Wang W., Lu C., Zhang Q. Study on the thermophysical properties and influencing factors of regional surface shallow rock and soil in China. *Frontiers in Earth Science*. 2022. Vol. 10. P. 864548. URL: https://doi.org/10.3389/feart.2022.864548. **22.** Petcu C., Dobrescu C. F., Dragomir C. S., Ciobanu A. A., Lăzărescu A. V., Hegyi A. Thermophysical Characteristics of Clay for Efficient Rammed Earth Wall Construction. *Materials*. 2023. Vol. 16. Issue 17. P. 6015. URL: https://doi.org/10.3390/ma16176015. **23.** Gorban V. A., Bilova N. A. Forest plantations influence on the thermophysical properties of southern chernozems. *Visnyk of V. N. Karazin Kharkiv National University. Series Ecology*. 2024. Issue 30. URL: https://doi.org/10.26565/1992-4259-2024-30-02. **24.** Vlasyuk A., Zhukovskyy V., Zhukovska N., Pinchuk O., Rajab H. Mathematical modeling of heat, mass, and moisture transfer in catalytic porous media. *WSEAS Transactions on Applied and Theoretical Mechanics*. 2020. May. URL: https://doi.org/10.37394/232011.2020.15.8. **25.** Nikiforova T., Savytskyi M., Limam K., Bosschaerts W., Belarbi R. Methods and results of experimental researches of thermal conductivity of soils. *Energy Procedia*. 2013. Vol. 42.

Pp. 775–783. URL: https://doi.org/10.1016/j.egypro.2013.12.034. **26.** Sadeghi M., Ghanbarian B., Horton R. Derivation of an explicit form of the percolation-based effective-medium approximation for thermal conductivity of partially saturated soils. *Water Resources Research*. 2018. Vol. 54. Pp. 1389–1399. URL: https://doi.org/10.1002/2017WR021714. **27.** Somerton W. H., El-Shaarani A. H., Mobarak S. M. High temperature behavior of rocks associated with geothermal type reservoirs. *Paper SPE-4897 presented at 44th Annual California Regional Meeting of the Society of Petroleum Engineers*. San Francisco, CA, 1974. URL: https://doi.org/10.2118/4897-MS

Шостак Л. В., аспірант (Національний університет водного господарства та природокористування, м. Рівне)

КОМП'ЮТЕРНЕ МОДЕЛЮВАННЯ РОЗПОДІЛУ ТЕМПЕРАТУРИ В ҐРУНТІ ЛІСУ З УРАХУВАННЯМ НАЯВНОСТІ ТОНКОГО ПРИМЕЖОВОГО ШАРУ ОПАЛОГО ЛИСТЯ

У статті розглянуто задачу чисельного моделювання розподілу температури в ґрунті лісової екосистеми з урахуванням впливу тонкого примежового шару опалого листя. Цей шар значно змінює теплопровідні властивості ґрунту, регулюючи теплообмін між атмосферою і підстилаючими шарами ґрунту. Для уточненого моделювання процесів теплообміну автор модифікувала граничну умову для рівняння теплопровідності, враховуючи фізичні характеристики лісової підстилки. Задля розв'язання відповідної крайової задачі використано метод скінченних різниць, що дозволяє врахувати варіативність теплопередачі в ґрунті. Чисельні експерименти показали значний вплив примежового шару опалого листя на динаміку температурних змін, що є важливим для оцінки екологічних процесів, удосконалення агротехнологій та прогнозування кліматичних змін в ґрунті. Отримані результати можуть бути застосовані для покращення розуміння теплових процесів у лісових екосистемах і розвитку нових підходів до екологічного моніторингу та моделювання кліматичних сценаріїв.

Ключові слова: **моделювання температури; ґрунт; лісова екосистема; опале листя; теплоізоляція; теплопередача; примежовий шар; метод скінченних різниць; вологість; температурний режим.**